The association between Hfq and RNase E in long-term nitrogen starved *Escherichia coli*

Josh McQuail[1], Agamemnon J. Carpousis[2] and Sivaramesh Wigneshweraraj[1*]

[1]MRC Centre for Molecular Bacteriology, Imperial College London, London, SW7 2AZ, UK.

[2] Laboratoire de Microbiologie et de Génétique Moléculaires (LMGM), Centre de Biologie Intégrative (CBI), Université de Toulouse, CNRS, UPS, Toulouse, France

*Correspondence: s.r.wig@imperial.ac.uk

Abstract

The regulation of bacterial gene expression is underpinned by the synthesis and degradation of mRNA. In *Escherichia coli*, RNase E is the central enzyme involved in RNA degradation and serves as a scaffold for the assembly of the multiprotein complex known as the RNA degradosome. The activity of RNase E against specific mRNAs can also be regulated by the action of small RNAs (sRNA). The ubiquitous bacterial chaperone Hfq bound to sRNAs interacts with the RNA degradosome for the sRNA guided degradation of target mRNAs. The association between RNase E and Hfq has never been observed in live bacteria. We now show that in long-term nitrogen starved *E. coli*, both RNase E and Hfq co-localise in a single, large focus. This subcellular assembly, which we refer to as the H-body, also includes components of the RNA degradosome, namely, the helicase RhlB and the exoribonuclease polynucleotide phosphorylase. We further show that H-bodies are important for *E. coli* to optimally survive sustained nitrogen starvation. Collectively, the properties and features of the H-body suggests that it represents a hitherto unreported example of subcellular compartmentalisation of a process(s) associated with RNA management in stressed bacteria.

1. Introduction

The synthesis and degradation of mRNA underpins the ability of bacteria to adapt the flow of genetic information to efficiently respond to specific environmental stimuli. In addition, non-coding small RNAs (sRNAs) contribute to the regulation of bacterial gene expression by acting as multitarget repressors and activators of gene expression. The binding of sRNAs to 5' untranslated regions of mRNAs can result in either mRNA stabilisation (leading to translation or translational repression) or degradation. In *Escherichia coli* and related bacteria, the endoribonuclease RNase E, an essential enzyme, is involved in the degradation of most mRNAs (1-3) and the biogenesis of sRNAs from the 3' untranslated regions of mRNAs (4-6). RNase E has a preference for 5' monophosphorylated RNA substrates and the RNA phosphohydrolase RppH converts 5' triphosphorylated mRNA into mRNA with 5' monophosphorylated ends. RNase E can also cleave RNA in a 5' end independent manner and genome-wide surveys of RNase E cleavage sites have revealed that this represents the major mRNA cleavage pathway in *E. coli* (4, 7). The catalytic domain of RNase E (amino acid residues 1-510) is located at the N terminus of the protein. The large noncatalytic carboxyl terminal region of RNase E (amino acid residues 511-1061) is intrinsically disordered and serves as the scaffold for the assembly of a multienzyme complex known as the RNA degradosome (8, 9). The RNA degradosome of *E. coli* consists of the DEAD-box helicase RhlB and the exoribonuclease polynucleotide phosphorylase (PNPase). Both PNPase and RNase E carry out RNA degradation and RhlB facilitates this by unwinding stem-loops within the RNA targets (1-3). The glycolytic enzyme enolase is an auxiliary component of the RNA degradosome and also interacts with carboxyl terminal region of RNase E; it is suspected to have a regulatory role in mRNA degradation in response to phosphosugar (10) and anaerobic

stress (11). Hence, for simplicity, we will refer to the RNA degradosome containing RNase E, RhlB and PNPase as the 'minimal' RNA degradosome complex.

The carboxyl terminal region of RNase E contains short amphipathic α-helix, called the membrane targeting sequence (MTS; amino acid residues 565-585), which allows it to interact with the inner cytoplasmic membrane of *E. coli* (12-14). Strahl *et al.*, showed that RNase E diffuses freely over the entire surface of the inner cytoplasmic membrane in exponentially growing *E. coli* cells but occasionally forms multiple short-lived puncta (15). This led the authors to suggest that the RNase E puncta either represented the RNA degradosome or a stable complex of the RNA degradosome with polysomes. Recently, Al-Husini *et al* showed that the α-proteobacterial RNase E of *Caulobacter crescentus*, which lacks an MTS, is located in the interior of the cell and assembles into liquid-liquid phase separated, short-lived clusters of 0.2-0.4 μm in diameter. These clusters, which are called BR-bodies, recruit RNA degradosome components (in this case RhlB and aconitase, which is the equivalent of enolase) particularly in stressed *C. crescentus* cells (16). In a subsequent study, Al-Husini et al showed that BR-bodies were specifically enriched in poorly translated mRNAs and sRNAs and functioned to promote efficient, most likely sRNA-guided (see below), degradation of mRNAs in stressed *C. crescentus* cells (17).

The ubiquitous bacterial chaperone Hfq bound to sRNAs can interact with RNase E for the sRNA-guided degradation of target mRNAs. This RNase E-Hfq/sRNA complex has been proposed to be distinct from the canonical minimal RNA degradosome (18). However, a study by Bruce et al used structural and biophysical approaches to provide evidence that Hfq/sRNA can interact with the RNA degradosome (19). It thus is yet possible that the interaction between Hfq/sRNA and RNase E and that of Hfq/sRNA with the RNA degradosome are mutually exclusive. Nevertheless, the importance of the sRNA guided association of Hfq with RNase E for targeted RNA degradation in *E. coli* and related bacteria is undisputed. However, the

association Hfq and RNase E has never been observed in live bacterial cells. Recently, we demonstrated that Hfq forms single, large (~0.3 µm), long-lived foci in long-term nitrogen (N) starved *E. coli* (20). In this study, we explored whether RNase E or the minimal RNA degradosome are constituents of the Hfq foci and thereby represent a compartmentalised subcellular assembly involved in RNA degradation in long-term N starved *E. coli*.

2. Results

2.1 RNase E assembles into a single, large focus in long-term N starved *Escherichia coli* cells

To determine whether RNase E associates with the Hfq foci in long-term N starved *E. coli*, we constructed an *E. coli* strain containing GFP and photoactivatable mCherry (PAmCherry) fused to the carboxyl terminal ends of *rne* and *hfq* at their normal chromosomal locations, respectively. Control experiments established that the ability of the Hfq-PAmCherry and RNase E-GFP tagged *E. coli* strain to survive long-term (24 h) N starvation did not differ from that of the untagged parent strain (Figure 1a). We initially studied the intracellular distribution of RNase E-GFP in exponentially growing bacteria under N replete conditions (N+), shortly following N run-out (~20 min starvation) in the growth media (N-) and in long-term N starved bacteria following 24 h of N starvation (N-24) by fluorescent microscopy using the experimental setup described by McQuail *et al.* (20). At N+ and N-, the majority of RNase E molecules were evenly distributed in the cell (Figure 1b and 1c). Consistent with previous observations (15), we also observed small clusters of RNase E proximal to the inner cytoplasmic membrane (Figure 1b and 1c). However, at N-24, we often observed a single, large cluster of RNase E, which we refer to as the RNase E focus, near the cell pole (Figure 1d). The RNase E foci were similar in size (~0.3 µm) as the Hfq foci that is also in 24 h N starved

bacteria (20). Notably, the RNase E foci were significantly larger than the multiple RNase E puncta previously observed in exponentially growing *E. coli* cells by Strahl et al (15). , Like the Hfq foci, the RNase E foci were observed in cells that were starved for N for up to 72 h (Supplementary Figure 1) and dispersed when the N starvation stress was alleviated by the addition of N (see later and (20)). Further, in a strain with a RNase E variant lacking the MTS (RNase $E_{\Delta 565\text{-}585}$), RNase E foci formation was unaffected (Figure 1e). This suggests that RNase E puncta observed previously (which requires inner membrane association (15)) and the RNase E foci observed under our conditions are physically different. Recently, we reported that despite running out of N at N-1, *E. coli* cells remain transcriptionally active with ~10% of the transcriptome differentially expressed (242 genes upregulated and 209 genes down regulated) specifically over the initial 24 h under N starvation (21). However, the depletion of cellular RNA levels by the addition of the transcription inhibitor rifampicin at N- did not have any detectable effect on Hfq foci formation at N-24 (20). Hence, we studied how the treatment of bacteria with rifampicin at N-, which will lead to the inhibition of *de novo* transcription and consequent depletion of cellular RNA pool over time, affected RNase E foci formation at N-24. As shown in Figure 1f, whereas rifampicin addition at N-, as expected, had no detectable effect on the efficacy of Hfq foci formation (20), no RNase E foci were detected at N-24. The loss of RNase E foci upon rifampicin treatment suggests that cellular RNA levels have a role in RNase E foci formation. Overall, we conclude that RNase E, like Hfq (20), forms a single and large focus, which is unlikely to be inner cytoplasmic membrane associated, in long-term N starved *E. coli*.

2.2 RNase E and Hfq foci colocalise in long-term N starved *Escherichia coli*

As the RNase E foci (Figure 1) resembles the Hfq foci (20) and the interaction between Hfq and RNase E/RNase E degradosome is undisputed, (1, 2, 4, 22), we investigated whether the RNase E and Hfq foci colocalise in long-term N starved *E. coli* cells. At N+ and N-, we only detected (if any at all) minimal overlap between RNase E and Hfq (Figure 2a and 2b). However, at N-24, the RNase foci clearly colocalised with the Hfq foci (Figure 2c). The colocalisation of the RNase E and Hfq foci persisted for at least 72 h under N starvation (Supplementary Figure 1). Previously we demonstrated that the Hfq foci dispersed when N starvation was alleviated (i.e., upon the addition of N to the *E. coli* cells at N-24) (20). We thus considered whether alleviation of N starvation would also cause the concomitant dispersion of the RNase E and Hfq foci. As shown in Figure 2d, this was indeed the case, and the results suggest that the formation of RNase E and Hfq foci are somehow linked. Corroborating this view, the formation of the RNase E and Hfq foci appeared to occur simultaneously as N starvation conditions ensued (Supplementary Figure 2). Further, the RNase E foci were undetectable in Δ*hfq E. coli* cells and reappeared when plasmid borne Hfq was supplied to Δ*hfq* bacteria (Figure 2e). Thus, it appears that the formation of the Hfq foci is a pre-requisite for the formation of the RNase E foci. Previously, Morita *et al.,* used affinity pull-down experiments to demonstrate that a truncated form of RNase E, lacking the majority of the carboxyl terminal region and thus consisting only of amino acid residues 1-700 (RNase $E_{1\text{-}700}$), failed to interact with Hfq (18). Consistent with this previous result mapping the RNase E region required for interaction with Hfq (23), and supporting the conclusions from results shown in Figure 2d and 2e, we failed to detect the RNase E foci in an *E. coli* strain in which RNase $E_{1\text{-}700}$ was fused to GFP, whereas the Hfq foci formation was unaffected (Figure 2f). Overall, we conclude that the formation of

the large RNase E foci seen in long-term N starved *E. coli* cells, is dependent upon and colocalises with the Hfq foci.

2.3. The involvement of RhlB and PNPase in the colocalisation of RNase E and Hfq foci in long-term N starved *E. coli* cells

As the minimal RNA degradosome of *E. coli* consists of PNPase and RhlB, we investigated whether PNPase and RhlB colocalised ~~of~~ to the RNase E/Hfq foci. Control experiments established that the ability of the Hfq-PAmCherry and PNPase-GFP and RhlB-GFP tagged *E. coli* strain to survive long-term (24 h) N starvation did not differ from that of the untagged parent strain (Supplementary Figure 3). As shown in Figure 3a and 3b, we observed distinct foci of PNPase and RhlB in *E. coli* cells from N-24, which, like the RNase E foci, colocalised with the Hfq foci. We next reasoned that if PNPase and RhlB were indeed part of the RNase E foci (because they interact with RNase E), then they would not form foci (and thus not colocalise with the Hfq foci) under conditions when the RNase E foci are absent. As the RNase E_{1-700} does not form the foci (and also does not contain the interaction sites for PNPase and RhlB) (Figure 2f), we thus investigated whether the RhlB and PNPase can form foci that colocalise with the Hfq foci in the *E. coli* strain containing RNase E_{1-700}. As shown in Figure 3c and 3d, respectively, we did not detect any distinct PNPase or RhlB foci in the *E. coli* strain containing the RNase E_{1-700} at N-24. However, as expected (Figure 2f), the formation of the Hfq foci was unaffected. The results thus indicate that the components of the minimal RNA degradosome are recruited by RNase E to the Hfq foci, which specifically form in long-term N starved *E. coli*. Further, as Hfq/sRNA also interacts with RNase E independently of the RNA degradosome, we investigated whether the co-localisation of RNase E and Hfq foci in long-term N starved *E. coli* is affected in anyway by the absence of either PNPase or RhlB. As

shown in Figure 3e and 3f, RNase E and Hfq foci formation and their colocalisation was unaffected in bacteria devoid of either PNPase or RhlB. Overall, it seems that a large spatiotemporally separated multiprotein complex, consisting of Hfq, RNase E, RhlB and PNPase, exists in long-term N starved *E. coli*. As the colocalisation of RNase E foci was dependent on the Hfq foci, we have referred to the colocalised feature as the H-body. We propose that the H-body is an important feature of the adaptive response to long-term N starvation. Consistent with this view, the absence of Hfq results in ~61% decrease in the proportion of viable cells at N-24 compared to the wild-type strain (Figure 3g and (20)) and we note that the *E. coli* strain harbouring the RNase E_{1-700} variant or lacking RhlB or PNPase (i.e. in cells where the H-body cannot form but the Hfq foci exists) display a similarly compromised (~50% of wild-type) viability at N-24 as the Δ*hfq E. coli* strain (Figure 3g).

2.4. H-bodies resemble liquid-liquid phase separated subcellular assemblies

Liquid-liquid phase separation (LLPS) is a ubiquitous mechanism by which cells form membraneless subcompartments. LLPS occurs when proteins and nucleic acids – often associated with a common biological process – make multiple transient and multivalent interactions that causes them to condense into a dense phase that resembles liquid droplets, that coexists with the dilute phase (24). Previously Al-Husini *et al.*, showed that RNase E of *C. crescentus* forms BR-bodies by LLPS (16). This precedence, together with our finding that RNase E, foci that form under our conditions, are unlikely to be anchored to the inner cytoplasmic membrane (Figure 1e), prompted us to consider whether H-body formation occurs by LLPS. Therefore, as the formation of the RNase E foci (and by extension the formation of PNPase and RhlB foci) are dependent of the formation of the Hfq foci (Figure 2e), we used the Hfq foci as a surrogate to determine whether H-bodies form by LLPS. Sensitivity to hexanediol

(HEX) - an aliphatic alcohol that disrupts subcellular assemblies that form by LLPS - is widely utilised as a useful, albeit not definitive, indicator of LLPS in bacterial cells (16, 25). Therefore, we treated *E. coli* cells from N-24, in which Hfq foci had formed, with HEX for 30 min. As shown in Figure 4a, the Hfq foci dispersed following the addition of HEX. However, they reassembled when the HEX was washed out of the culture. Consistent with the observation that the formation of the RNase E foci is dependent on the Hfq foci, the RNase E foci also dispersed following HEX treatment (Figure 4b). Overall, we conclude that the H-bodies in long-term N starved *E. coli* cells physically resemble LLPS subcellular assemblies.

3. Discussion

The importance of the association between RNase E and Hfq to the post-transcriptional fate of RNA in bacteria is undisputed. We recently reported that Hfq molecules cluster into a large focus-like structure in long-term N starved *E. coli* (20). Although we demonstrated that the Hfq foci are important for *E. coli* to adapt to long-term N starvation, their composition and mechanistic details of their biological role remain elusive. In this study, we focused on the composition of the Hfq foci. Prompted by the established associations between Hfq/sRNA and the RNA degradosome in *E. coli* (18, 19) and the recent discovery that the RNA degradosome can form foci-like assemblies in *C. crescentus* (16, 17), we focused our analysis to investigate whether the Hfq foci contained components of the RNA degradosome. Indeed, we have demonstrated that RNase E, PNPase and RhlB, which constitute the minimal RNA degradosome in *E. coli*, colocalise with the Hfq foci - the H body. Further, to the best of our knowledge, this is the first time that an association between Hfq and the RNA degradosome has been visualised in live bacteria. As RNase E and Hfq colocalise even in mutant bacteria devoid of either PNPase or RhlB, it is plausible (but impossible to decipher from our

experiments) that H-bodies consists of (at least) two mutually exclusive multiprotein complexes, namely, Hfq/sRNA and RNase E and Hfq/sRNA and the minimal RNA degradosome.

Remarkably, the size (~0.3 µm in diameter), behaviour (dispersion when stress is alleviated), longevity and physical properties (formation by LLPS like mechanism) of the H-bodies bear similarities to the BR-bodies seen in α-proteobacteria (16, 17) and analogous assemblies in stressed eukaryotic cells, such as P bodies or stress granules (26). As P-bodies and stress granules are sites of RNA storage and turnover in stressed eukaryotic cells, based on the observation that the depletion of total cellular RNA affects H-body formation (Figure 1f), we propose that RNA is a constituent of the H-bodies. As previously reported by us, due to the poor permeability of bacteria at N-24, attempts to stain the H-bodies with RNA specific stains were unsuccessful (20). Overall, we propose that the H-bodies, like BR-bodies of *C. crescentus*, could serve to physically separate sRNA-induced mRNA degradation from other cellular processes in long-term N starved *E. coli* cells.

Membraneless compartmentalisation of RNA associated processes by LLPS is emerging to be pervasive in bacteria and, in addition to BR-bodies in α-proteobacteria, the RNA polymerase has also been shown to undergo LLPS in *E. coli* (27). Our results suggest that the H-bodies could represent 'membraneless compartments' determining the post-transcriptional fate of RNA in long-term N starved *E. coli* cells. The fact that H-bodies disperse when the N starvation stress is alleviated (Figure 2e) and their absence compromises viability of long-term N starved *E. coli* (Figure 3g) suggests that H-bodies contribute to the adaptive response of *E. coli* to N starvation (although, we cannot rule out the possibility that the apparent decrease in viability is also due to non-H-body related activities of Hfq, PNPase, RhlB or the functionally compromised RNase E_{1-700} variant in N starved *E. coli*). It is conceivable that the H-bodies form to efficiently degrade untranslated mRNAs and rRNAs in N starved *E. coli* to

release N from nitrogenous RNA molecules to maintain cellular processes as N starvation ensues. In support of this view, we recently reported that 16S and 23S rRNAs are gradually degraded over the initial 24 h under N starvation, i.e., over a period of time that coincides with H-body formation (21). Hfq is involved in the assembly of ribosomes (28) and recently it was reported that Hfq, together with the 3'-5' exoribonuclease RNase R, is involved in the degradation pathway associated with the removal of abnormal rRNA intermediates (29). Thus, it is plausible that H-bodies are associated with the degradation of 16S and 23S rRNAs during long-term N starvation. Consistent with this view, it seems that the degradation of 16S and 23S rRNAs in long-term N starved *E. coli* is dependent on Hfq as the efficiency of rRNA degradation is significantly compromised in the Δ*hfq E. coli* strain (Supplementary Figure 4a, 4b and 4e). It seems that the potential involvement of Hfq in the ribosome degradation pathway is specific to N starvation as it is not seen in long-term carbon starved *E. coli* (Supplementary Figure 4c, 4d and 4e). This observation is in line with the fact Hfq foci, i.e., H-bodies, do not form in long-term carbon starved *E. coli* (20). Therefore, H-body formation could be a mechanism to spatially separate and enable rapid degradation of untranslated mRNAs and rRNAs to manage metabolism specifically in long-term N starved *E. coli* cells to ensure viability. However, in regard to the latter, as RNase R appears not to be a constituent of the H-body (Supplementary Figure 5), at this point, we can't be certain whether RNA degradation in long-term N starved *E. coli* is an Hfq dependent property that happens outside of the H-body.

Interestingly, the intrinsically disordered region of RNA binding proteins is often necessary for LLPS in both eukaryotic and prokaryotic systems. In fact, the RNase E of *C. crescentus* requires its intrinsically disordered carboxyl terminal region to undergo LLPS and form BR-bodies (16). Our data demonstrates that Hfq foci formation is a requirement for RNase E foci to form and colocalise with the Hfq foci, i.e., formation of H-bodies. Intriguingly, the intrinsically disordered carboxyl terminal region of Hfq is not required for Hfq foci

formation (20). However, the RNAse E_{1-700}, which lacks its intrinsically disordered region, is unable to form foci. This could suggest that the intrinsically disordered region of RNase E might be required for foci formation by LLPS and association with the Hfq foci. However, at this stage, we cannot exclude the possibility that the inability of RNase E to interact with Hfq (because it is lacking the carboxyl terminal region), rather than the absence of the intrinsically disordered region *per se*, is the contributing factor for the inability of RNase E_{1-700} to form the foci. Therefore, it is possible that H-body formation by LLPS and the physical~~ly~~ properties of H-bodies are influenced by other, yet to be identified, interacting partners. Although we will next focus on identifying the RNA and protein components of H-bodies, in an unbiased manner at the genome-wide scale, this study has uncovered that undergoing LLPS to form large 'compartmentalised' membraneless subcellular assemblies is a hitherto unreported property of the ubiquitous bacterial RNA chaperone Hfq.

4. Experimental Procedures

Bacterial strains and plasmids. All strains used in this study were derived from *Escherichia coli* K-12 and are listed in Supplementary Table 1. The Hfq-PAmCherry was made as previously described (20). Tagged genes (*rne*-msfGFP, *rne*(Δ565−585)-eGFP, *rne*700-msfGFP, *pnp*-msfGFP, *rhlB*-msfGPF and *rnr*-msfGFP) and gene deletions (Δ*hfq*, Δ*pnp* and Δ*rhlB*) were introduced into the *E. coli* strain containing Hfq-PAmCherry and derivative strains as described previously (30). Briefly the tagged or knockout alleles were transduced using the P1vir bacteriophage from the appropriate donor strains listed in Table 1. The *rne*-msfGFP strain (SAJ232) and *rne700*-msfGFP strains (SAJ233) were constructed as described previously (15).

Bacterial growth conditions. Bacteria were grown in Gutnick minimal medium (33.8 mM KH_2PO_4, 77.5 mM K_2HPO_4, 5.74 mM K_2SO_4, 0.41 mM $MgSO_4$) supplemented with Ho-LE trace elements (31), 0.4% (w/v) glucose as the sole C source and NH_4Cl as the sole N source. Overnight cultures were grown at 37 °C, 180 r.p.m. in Gutnick minimal medium containing 10 mM NH_4Cl. For the N starvation experiments, 3 mM NH_4Cl was used. The proportion of viable cells in the bacterial population was determined by measuring CFU/ml from serial dilutions on lysogeny broth agar plates. To observe Hfq and RNase E foci dissipation, 25 ml of the 24 h N starved culture was centrifuged at 3,200 *g* and resuspend in fresh Gutnick minimal medium containing 0.4% (w/v) glucose and 3 mM NH_4Cl and grown at 37 °C, 180 r.p.m. for 3 hours. For carbon starvation experiments, bacteria were grown in Gutnick minimal medium containing 22 mM glucose and 10 mM NH_4Cl as previously described (20).

Microscopy. For the PALM experiments, the bacterial cultures were grown as described above and samples were taken at the indicated time points, then imaged and analysed as previously described (32, 33). Briefly, 1 ml of culture was centrifuged, washed and resuspended in a small amount of Gutnick minimal medium without any NH_4Cl; samples taken at N+ were resuspended in Gutnick minimal medium with 3 mM NH_4Cl. One microlitre of the resuspended culture was then placed on a Gutnick minimal medium agarose pad (1x Gutnick minimal medium without any NH_4Cl with 1% (w/v) agarose); samples taken at N+ were placed on a pad made with Gutnick minimal medium with 3 mM NH_4Cl. Cells were imaged on a PALM-optimized Nanoimager (Oxford Nanoimaging, www.oxfordni.com) with 15 millisecond exposures, at 66 frames per second over 10,000 frames. Photoactivatable molecules were activated using 405 nm and 561 nm lasers. GFP images were acquired as above, except using

only a 488 nm laser, with single, 15-100 millisecond exposures, depending on GFP levels within the cell.

Total RNA analysis. Cultures were grown as described above and sampled at the following time points: during exponential growth (N+, C+) at the onset of starvation (N−, C-) and 24 h under starvation (N-24, C-24), during N and carbon starvation respectively. At least three biological replicates were taken at each time point. Cell samples were acquired and stabilized at specified time points using Qiagen RNA Protect reagent (76526; Qiagen). RNA extractions were performed using the PureLink RNA minikit (12183025; Invitrogen) and DNase set (12185010; Invitrogen) according to the manufacturers' protocols. Electropherograms of total RNA integrity were generated using an Agilent Bioanalyzer 2100 instrument (G2939BA; Agilent) and RNA 6000 Nano kit (5067-1511; Agilent) per the manufacturer's protocol.

Acknowledgements

We thank Lynn Burchell and Leonora Poljak who helped produce some of data and *E. coli* strains. This work was supported by grants from the Wellcome Trust (100958), Leverhulme Trust (RPG-2020-050) and BBSRC (BB/V000284/1) to SW. We thank Amy Switzer and Aline Tabib-Salazar for comments on the manuscript.

Author Contributions

Experimental design and planning (JM and SW), production and analysis of data (JM and SW), preparation of the manuscript (SW, JM, AJC).

1. S. Ait-Bara, A. J. Carpousis, RNA degradosomes in bacteria and chloroplasts: classification, distribution and evolution of RNase E homologs. *Mol Microbiol* **97**, 1021-1135 (2015).
2. K. J. Bandyra, M. Bouvier, A. J. Carpousis, B. F. Luisi, The social fabric of the RNA degradosome. *Biochim Biophys Acta* **1829**, 514-522 (2013).
3. D. A. Vargas-Blanco, S. S. Shell, Regulation of mRNA Stability During Bacterial Stress Responses. *Front Microbiol* **11**, 2111 (2020).
4. Y. Chao *et al.*, In Vivo Cleavage Map Illuminates the Central Role of RNase E in Coding and Non-coding RNA Pathways. *Mol Cell* **65**, 39-51 (2017).
5. Y. Chao, J. Vogel, A 3' UTR-Derived Small RNA Provides the Regulatory Noncoding Arm of the Inner Membrane Stress Response. *Mol Cell* **61**, 352-363 (2016).
6. Y. Chao, K. Papenfort, R. Reinhardt, C. M. Sharma, J. Vogel, An atlas of Hfq-bound transcripts reveals 3' UTRs as a genomic reservoir of regulatory small RNAs. *The EMBO journal* **31**, 4005-4019 (2012).
7. J. E. Clarke, L. Kime, A. D. Romero, K. J. McDowall, Direct entry by RNase E is a major pathway for the degradation and processing of RNA in Escherichia coli. *Nucleic Acids Res* **42**, 11733-11751 (2014).
8. A. J. Callaghan *et al.*, Structure of Escherichia coli RNase E catalytic domain and implications for RNA turnover. *Nature* **437**, 1187-1191 (2005).
9. A. J. Callaghan *et al.*, Studies of the RNA degradosome-organizing domain of the Escherichia coli ribonuclease RNase E. *J Mol Biol* **340**, 965-979 (2004).
10. V. Chandran, B. F. Luisi, Recognition of enolase in the Escherichia coli RNA degradosome. *J Mol Biol* **358**, 8-15 (2006).
11. O. N. Murashko, S. Lin-Chao, Escherichia coli responds to environmental changes using enolasic degradosomes and stabilized DicF sRNA to alter cellular morphology. *Proc Natl Acad Sci U S A* **114**, E8025-E8034 (2017).
12. A. Taghbalout, L. Rothfield, RNaseE and the other constituents of the RNA degradosome are components of the bacterial cytoskeleton. *Proc Natl Acad Sci U S A* **104**, 1667-1672 (2007).
13. A. Taghbalout, Q. Yang, V. Arluison, The Escherichia coli RNA processing and degradation machinery is compartmentalized within an organized cellular network. *Biochem J* **458**, 11-22 (2014).
14. V. Khemici, L. Poljak, B. F. Luisi, A. J. Carpousis, The RNase E of Escherichia coli is a membrane-binding protein. *Mol Microbiol* **70**, 799-813 (2008).
15. H. Strahl *et al.*, Membrane recognition and dynamics of the RNA degradosome. *PLoS Genet* **11**, e1004961 (2015).
16. N. Al-Husini, D. T. Tomares, O. Bitar, W. S. Childers, J. M. Schrader, alpha-Proteobacterial RNA Degradosomes Assemble Liquid-Liquid Phase-Separated RNP Bodies. *Molecular cell* **71**, 1027-1039 e1014 (2018).
17. N. Al-Husini *et al.*, BR-Bodies Provide Selectively Permeable Condensates that Stimulate mRNA Decay and Prevent Release of Decay Intermediates. *Molecular cell* **78**, 670-682 e678 (2020).
18. T. Morita, K. Maki, H. Aiba, RNase E-based ribonucleoprotein complexes: mechanical basis of mRNA destabilization mediated by bacterial noncoding RNAs. *Genes Dev* **19**, 2176-2186 (2005).

19. H. A. Bruce *et al.*, Analysis of the natively unstructured RNA/protein-recognition core in the Escherichia coli RNA degradosome and its interactions with regulatory RNA/Hfq complexes. *Nucleic Acids Res* **46**, 387-402 (2018).
20. J. McQuail, A. Switzer, L. Burchell, S. Wigneshweraraj, The RNA-binding protein Hfq assembles into foci-like structures in nitrogen starved Escherichia coli. *J Biol Chem* **295**, 12355-12367 (2020).
21. A. Switzer, L. Burchell, J. McQuail, S. Wigneshweraraj, The Adaptive Response to Long-Term Nitrogen Starvation in Escherichia coli Requires the Breakdown of Allantoin. *J Bacteriol* **202** (2020).
22. J. Vogel, B. F. Luisi, Hfq and its constellation of RNA. *Nat Rev Microbiol* **9**, 578-589 (2011).
23. Y. Ikeda, M. Yagi, T. Morita, H. Aiba, Hfq binding at RhlB-recognition region of RNase E is crucial for the rapid degradation of target mRNAs mediated by sRNAs in Escherichia coli. *Molecular microbiology* **79**, 419-432 (2011).
24. S. Alberti, A. Gladfelter, T. Mittag, Considerations and Challenges in Studying Liquid-Liquid Phase Separation and Biomolecular Condensates. *Cell* **176**, 419-434 (2019).
25. A. M. Ladouceur *et al.*, Clusters of bacterial RNA polymerase are biomolecular condensates that assemble through liquid-liquid phase separation. *Proc Natl Acad Sci U S A* 10.1073/pnas.2005019117 (2020).
26. Y. Luo, Z. Na, S. A. Slavoff, P-Bodies: Composition, Properties, and Functions. *Biochemistry* **57**, 2424-2431 (2018).
27. A. M. Ladouceur *et al.*, Clusters of bacterial RNA polymerase are biomolecular condensates that assemble through liquid-liquid phase separation. *Proceedings of the National Academy of Sciences of the United States of America* **117**, 18540-18549 (2020).
28. J. M. Andrade, R. F. Dos Santos, I. Chelysheva, Z. Ignatova, C. M. Arraiano, The RNA-binding protein Hfq is important for ribosome biogenesis and affects translation fidelity. *The EMBO journal* **37** (2018).
29. R. F. Dos Santos, J. M. Andrade, J. Pissarra, M. P. Deutscher, C. M. Arraiano, Hfq and RNase R Mediate rRNA Processing and Degradation in a Novel RNA Quality Control Process. *mBio* **11** (2020).
30. D. R. Brown, G. Barton, Z. Pan, M. Buck, S. Wigneshweraraj, Nitrogen stress response and stringent response are coupled in Escherichia coli. *Nature communications* **5**, 4115 (2014).
31. R. M. Atlas, *Handbook of Microbiological Media, Fourth Edition* (CRC Press, 2010).
32. M. Stracy *et al.*, Live-cell superresolution microscopy reveals the organization of RNA polymerase in the bacterial nucleoid. *Proceedings of the National Academy of Sciences of the United States of America* **112**, E4390-4399 (2015).
33. U. Endesfelder *et al.*, Multiscale spatial organization of RNA polymerase in Escherichia coli. *Biophysical journal* **105**, 172-181 (2013).

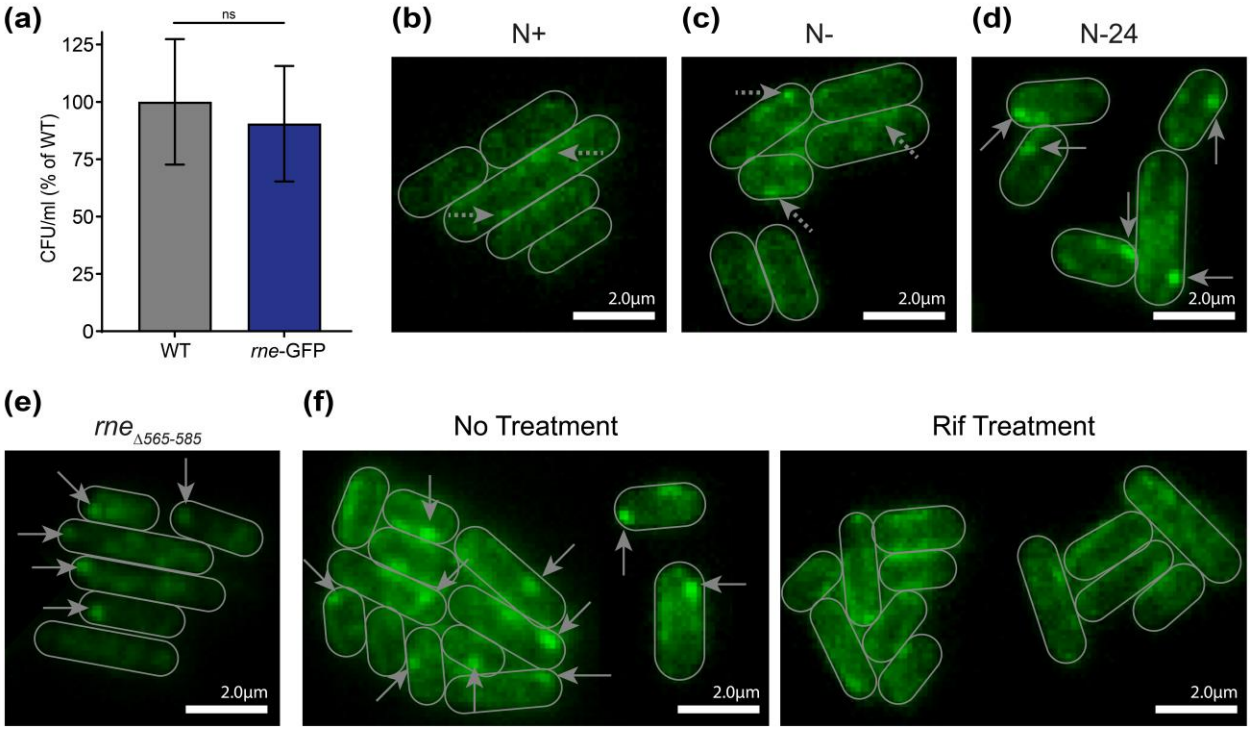

Figure 1. RNase E assembles into a single and large focus in long-term N starved *E. coli* cells. (a) Graph showing the proportion of viable cells in cultures of 24 h N starved WT and RNAse E-GFP (*rne*-GFP) containing *E. coli*, measured by counting CFU and shown as a percentage of WT. Error bars represent standard deviation (n = 3). (b, c, d) Representative fluorescence microscopy images of the distribution of RNase E in *E. coli* cells from (b) N+, (c) N- and (d) N-24. (e) Representative fluorescence microscopy image of RNase $E_{\Delta 565\text{-}585}$ ($rne_{\Delta 565\text{-}585}$) in 24 h N starved *E. coli* cells. (f) Representative fluorescence microscopy images of the distribution of RNase E in untreated and rifampicin (Rif; 100µg/ml) treated (at N-) *E. coli* cells imaged at N-24. In (b and c), the dashed arrows indicate previously described RNase E puncta. In (d, e and f), the solid arrows indicate the RNase E foci.

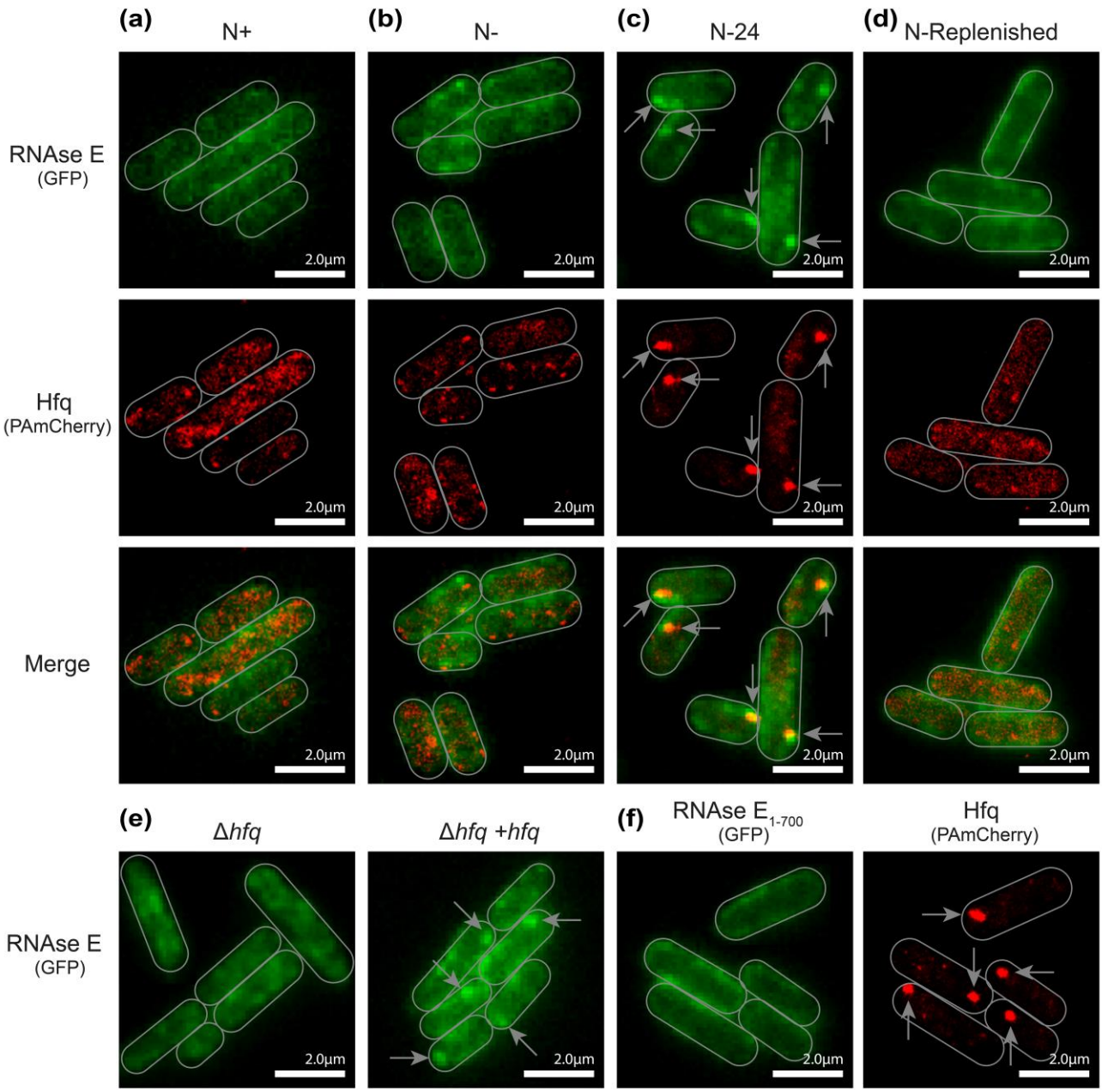

Figure 2. The RNase E and Hfq foci colocalise in long-term N starved *E. coli* cells. (a, b, c, d) Representative fluorescence microscopy (for RNase E), PALM (for Hfq) and merged images of RNase E and Hfq in *E. coli* cells, taken at (a) N+, (b) N-, (c) N-24 and (d) 3 h after 24 h N starved bacteria were replenished with N. (e) Representative fluorescence microscopy images of RNase E in 24 h N starved Δ*hfq* and Δ*hfq*+pBAD24-*hfq*-FLAG *E. coli* cells. (f) Representative fluorescence microscopy and PALM images of RNase E and Hfq in 24 h N starved *E. coli* cells containing RNase$_{1\text{-}700}$ (*rne*$_{1\text{-}700}$). In all figures, the arrows indicate the RNase E and/or Hfq foci.

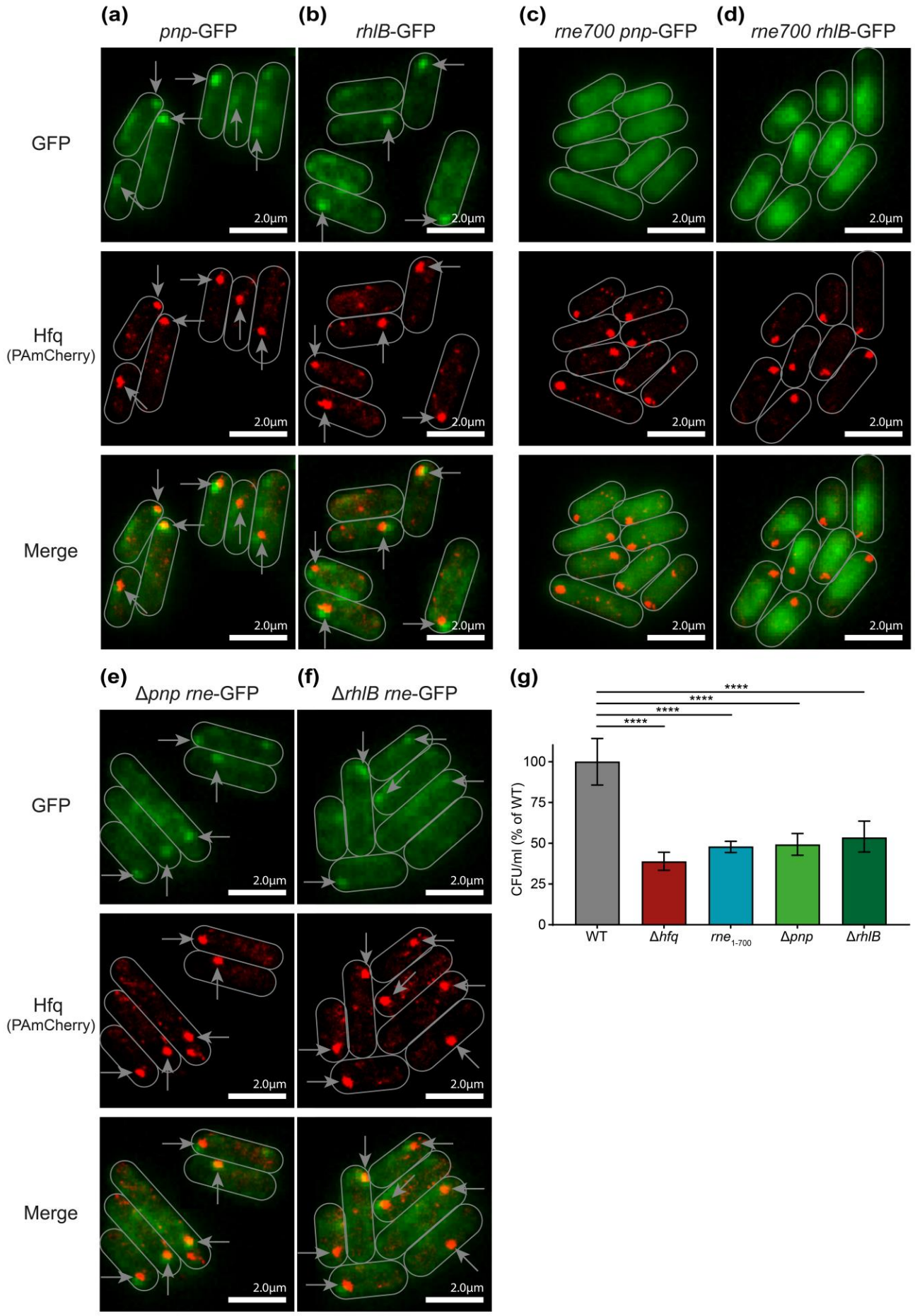
(a)
pnp-GFP
(b)
rhlB-GFP
(c)
rne700 pnp-GFP
(d)
rne700 rhlB-GFP
GFP
Hfq
(PAmCherry)
Merge
2.0µm
(e)
Δpnp rne-GFP
(f)
ΔrhlB rne-GFP
(g)
****
CFU/ml (% of WT)
100
75
50
25
0
WT
Δhfq
rne1-700
Δpnp
ΔrhlB

Figure 3. The involvement of RhlB and PNPase in the colocalisation of RNase E and Hfq foci in long-term N starved *E. coli* cells. (a, b) Representative fluorescence microscopy (for PNPase and RhlB), PALM (for Hfq) and merged images of (a) PNPase or (b) RhlB and Hfq in 24 h N starved *E. coli* cells. (c, d) Representative fluorescence microscopy (for PNPase and RhlB) and PALM (for Hfq) images of (c) PNPase or (d) RhlB and Hfq in 24 h N starved *E. coli* cells containing RNase $E_{1\text{-}700}$ ($rne_{1\text{-}700}$). (e, f) Representative fluorescence microscopy (for RNase E), PALM (for Hfq) and merged images of RNase E and Hfq in 24 h N starved *E. coli* cells devoid of (a) PNPase (Δ*pnp*) and (b) RhlB (Δ*rhlB*) cells. The arrows indicate the RNase E, PNPase, RhlB and/or Hfq foci. (g) Graph showing the proportion of viable cells in cultures of 24 h N starved WT, Δ*hfq*, $rne_{1\text{-}700}$, Δ*pnp* and Δ*rhlB E. coli* measured by counting CFU and shown as a percentage of WT. Error bars represent standard deviation (n = 3). Asterisks indicate significant differences between strains (****: $p < 0.0001$).

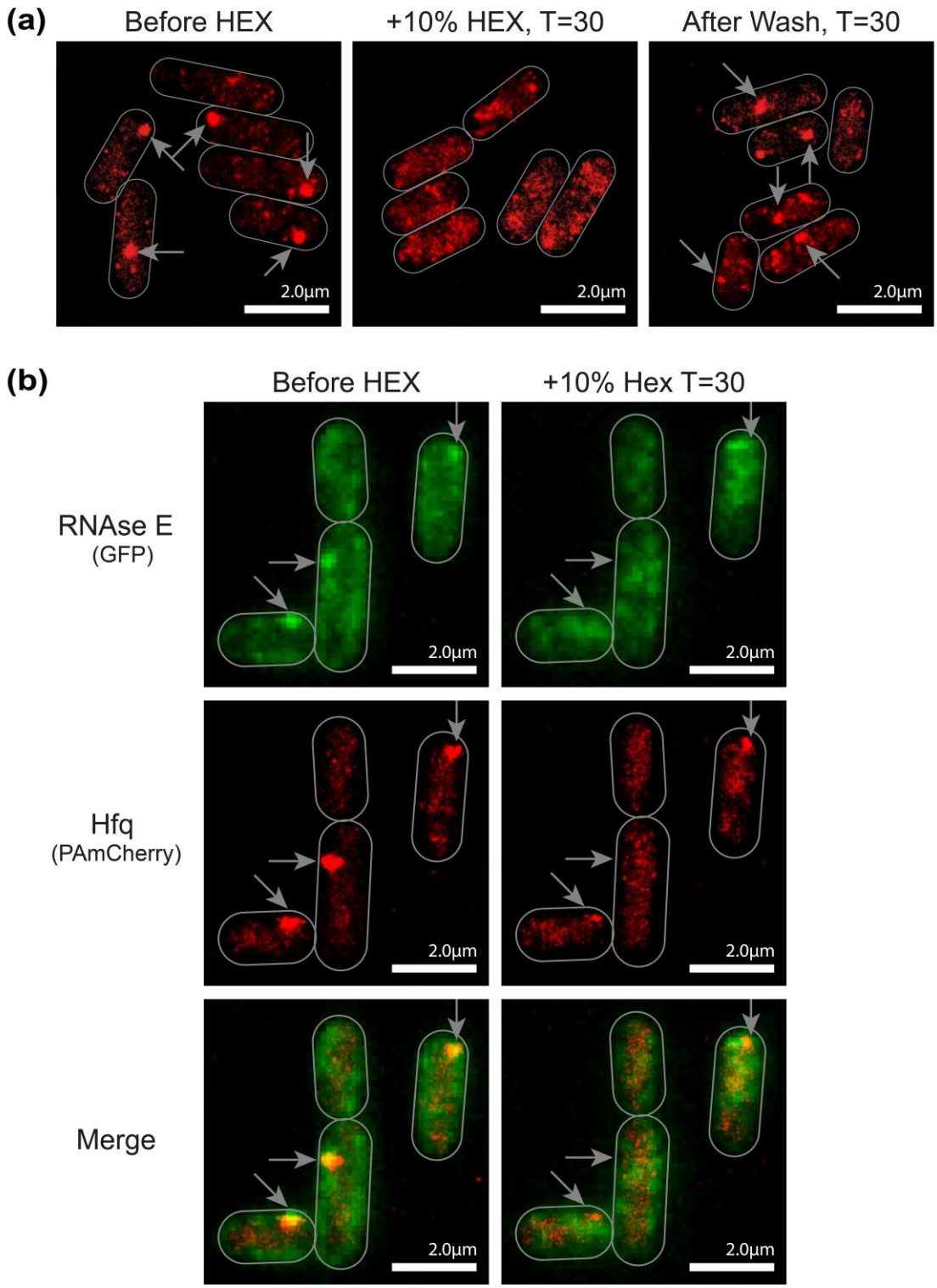

Figure 4. H-bodies resemble liquid-liquid phase separated subcellular assemblies. (a) Representative PALM images of Hfq in 24 h N starved *E. coli* cells before (left), after (middle) 30 min treatment with 10% (v/v) hexanediol and 30 min after removal of hexanediol from the culture (right). (b) Representative fluorescence microscopy (for RNase E), PALM (for Hfq) and merged images of RNase E and Hfq in 24 h N starved *E. coli* cells before and after 30 min treatment with 10% (v/v) hexanediol. The arrows indicate the RNase E and/or Hfq foci.

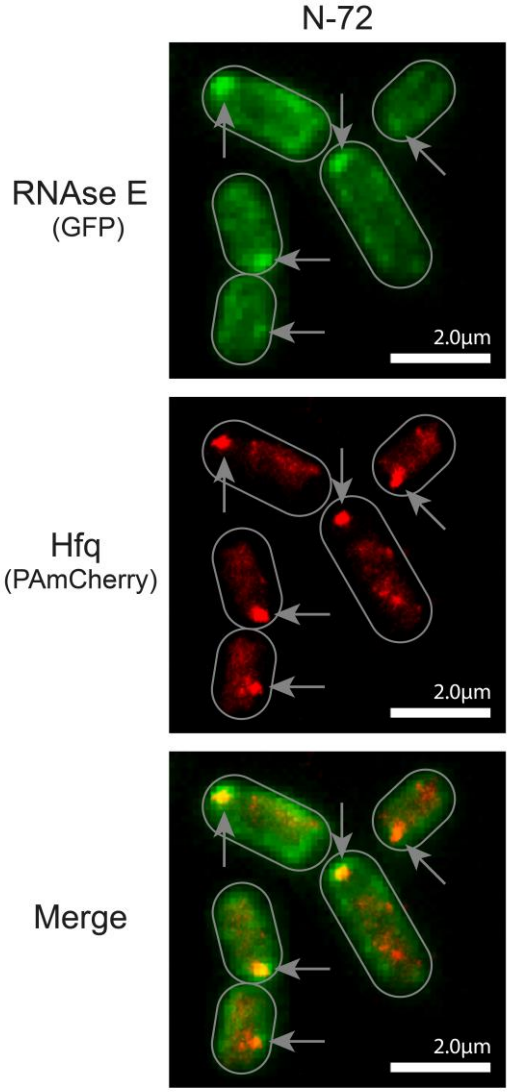

Supplementary Figure 1. The RNase E foci persist for up to 72 h. Representative fluorescence microscopy (for RNase E), PALM (for Hfq) and merged images of RNase E and Hfq in 72 h N starved *E. coli* cells.

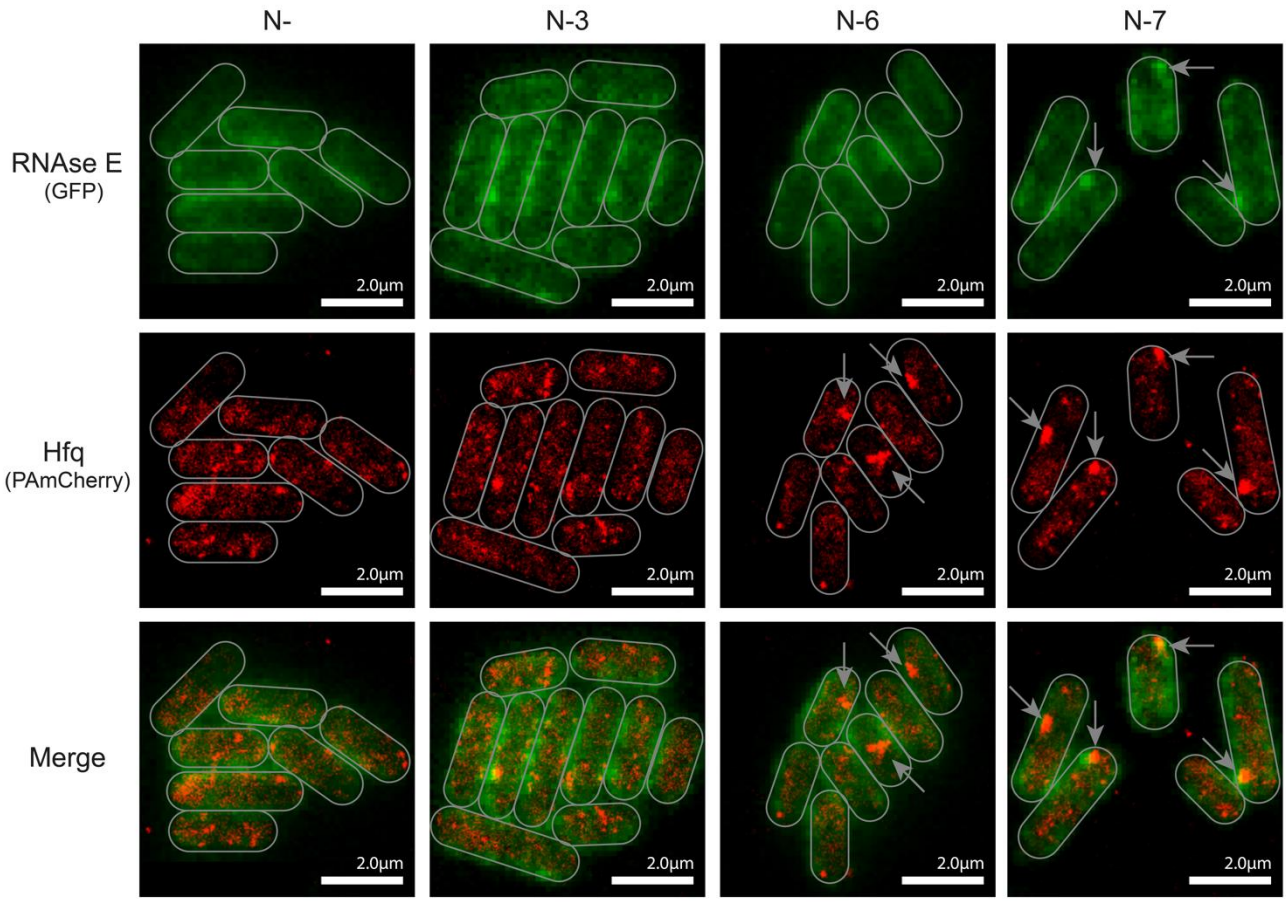

Supplementary Figure 2. The RNase E foci and Hfq foci form gradually and concomitantly. Representative fluorescence microscopy (for RNase E), PALM (for Hfq) and merged images of RNase E and Hfq in short-term, 3h, 6h and 7h N starved *E. coli* cells.

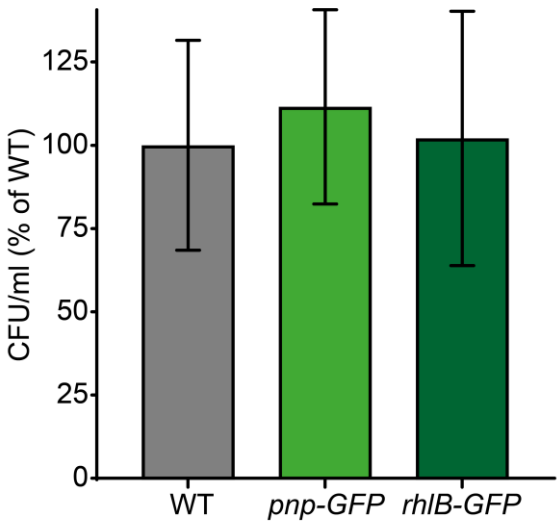

Supplementary Figure 3. Graph showing the proportion of viable cells in cultures of 24 h N starved WT, PNPase-GFP (*pnp*-GFP) and RhlB-GFP (*rhlB*-GFP) containing *E. coli*, measured by counting CFU and shown as a percentage of WT. Error bars represent standard deviation (n = 3).

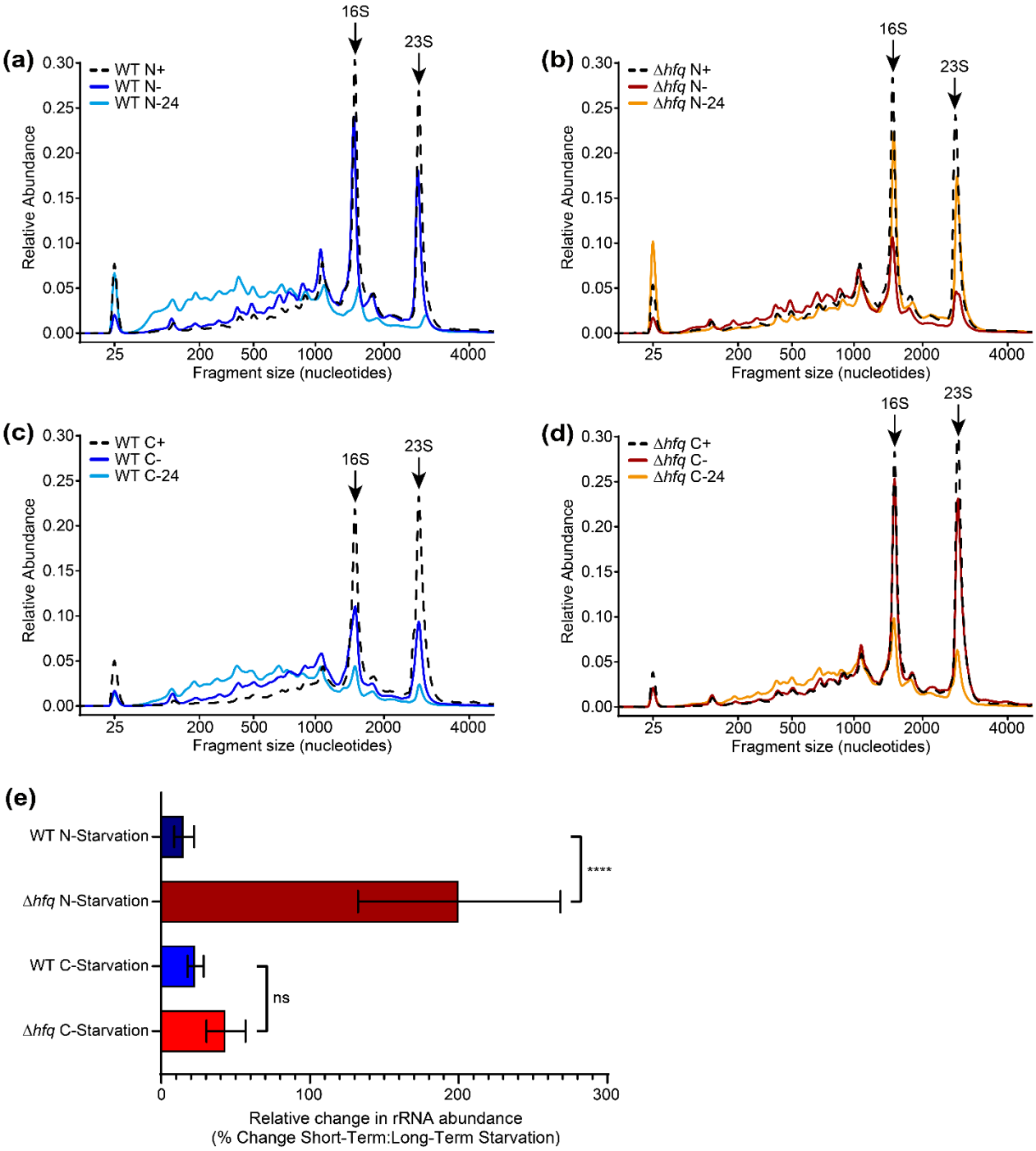

Supplementary Figure 4. (a,b,c,d) Electropherograms of total RNA extracted from WT (a,b) and Δ*hfq* (b,d) *E. coli* starved of either N (a,b) or carbon (c,d) growth, sampled at the indicated time points. Graphs represent the mean RNA profile, from at least three biological replicates. Data standardised by total RNA concentration from each sample. The 16S and 23S rRNA peaks are indicated. The peak at 25 nucleotides is a standard marker and can be ignored. (e) Graph showing change in relative rRNA abundance of total RNA extracted from WT and Δ*hfq* *E. coli* between short-term (N-, C-) and long-term (N-24, C-24) starvation time points. Relative rRNA abundance at long-term starvation time points are shown as a percentage of relative rRNA abundance at short-term starvation time points. Error bars represent standard deviation. Asterisks indicate significant differences between strains (****: $p < 0.0001$).

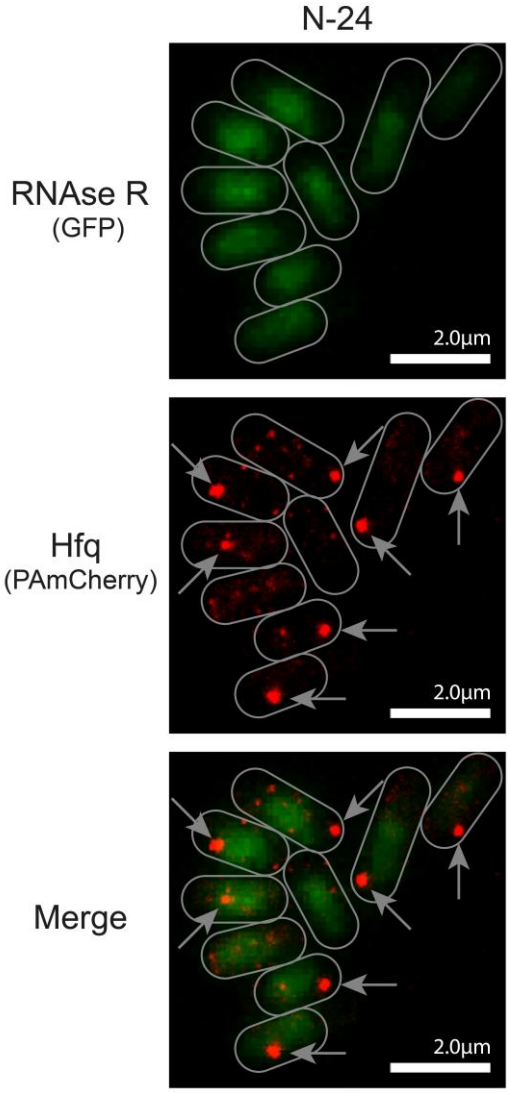

Supplementary Figure 5: RNase R do not co-localise with H-bodies. Representative fluorescence microscopy (for RNase R), PALM (for Hfq) and merged images of RNase R and Hfq in 24 h N starved *E. coli* cells.

Supplementary Table 1. - *E. coli* strains and plasmids used in this study

Strains		
Name	Description	Source or Reference
Wild-type MG1655	*E. coli* K-12 *rph*-1	E. coli Genetic Stock Centre
Wild-type (BW25113)	*E. coli* K-12 (*araD-araB*)567 Δ(*rhaD-rhaB*) 568 Δ*lac*Z4787 (*::rrnB-3*) *hsdR*514 *rph*-1	E. coli Genetic Stock Centre
Rne-msfGFP (SAJ232)	NCM3416 *rne(1-1061)-msfGFP-cat*	This study
RneΔMTS-eGFP (Kti491)	NCM3416 *rne(Δ 565-585)-efGFP-cat*	(15)
Hfq-PAmCherry	MG1655 *hfq-PAmCherry-kan*	(20)
Rne-msfGFP Hfq-PAmCherry	MG1655 *rne(1-1061)-msfGFP-cat hfq-PAmCherry-kan*	This Study
RneΔ565-585-eGFP Hfq-PAmCherry	MG1655 *rne(Δ565-585)-efGFP -cat hfq-PAmCherry-kan*	This Study
Δ*hfq* (JW4130)	BW25113 Δ*hfq::kan*	E. coli Genetic Stock Centre
Δ*hfq* Rne-msfGFP	MG1655 Δ*hfq::kan rne(1-1061)-msfGFP-cat*	This Study
Rne700-msfGFP (SAJ233)	NCM3416 *rne(1-700)-msfGFP-cat*	This study
Rne700-msfGFP Hfq-PAmCherry	MG1655 *rne(1-700)-msfGFP-cat hfq-PAmCherry-kan*	This Study
Δ*pnp* (JW5851)	BW25113 Δ*pnp::kan*	E. coli Genetic Stock Centre
Δ*rhlb* (JW3753)	BW25113 Δ*rhlb::kan*	E. coli Genetic Stock Centre
Δ*pnp* Rne-msfGFP Hfq-PAmCherry	MG1655 *rne(1-1061)-msfGFP-cat hfq-PAmCherry* Δ*pnp::kan*	This Study
Δ*rhlb* Rne-msfGFP Hfq-PAmCherry	MG1655 *rne(1-1061)-msfGFP-cat hfq-PAmCherry* Δ*rhlb::kan*	This Study
Pnp-msfGFP (SLM013)	NCM3416 *pnp-msfGFP-cat*	Gift from Lina Hamouche
RhlB-msfGFP (SLM021)	NCM3416 *rhlB-msfGFP-cat*	Gift from Lina Hamouche
Pnp-msfGFP Hfq-PAmCherry	MG1655 *pnp-msfGFP-cat hfq-PAmCherry-kan*	This Study
RhlB-msfGFP Hfq-PAmCherry	MG1655 *rhlB-msfGFP-cat hfq-PAmCherry-kan*	This Study
Rne701-FLAG (TM528)	W3110mic *rne(1-701)-Flag-cat*	(18)
Rne701-FLAG Pnp-msfGFP Hfq-PAmCherry	MG1655 *rne(1-701)-Flag-cat pnp-msfGFP hfq-PAmCherry-kan*	This Study
Rne701-FLAG RhlB-msfGFP Hfq-PAmCherry	MG1655 *rne(1-701)-Flag-cat rhlB-msfGFP hfq-PAmCherry-kan*	This Study
Rnr-msfGFP Hfq-PAmCherry	MG1655 *rnr-msfGFP-cat hfq-PAmCherry-kan*	This Study

Plasmids		
Name	Description	Source or Reference
pBAD24-*hfq*-FLAG	pBAD24 expressing *hfq*-3xFLAG under an arabinose inducible promoter	Gift from Jörg Vogel